



Contents lists available at ScienceDirect

Spectrochimica Acta Part A: Molecular and Biomolecular Spectroscopy

journal homepage: www.journals.elsevier.com/spectrochimica-acta-part-a-molecular-and-biomolecular-spectroscopy



Spectral and stiffness characterization of whole prostate gland to assist superficial cancer detection during radical prostatectomy

Olof Lindahl^{a,*}, András Gorzsás^b, Anders Bergh^c, Britt M. Andersson^d, Börje Ljungberg^e, Göran Mannberg^a, Per Liv^f, Tomas Bäcklund^a, Urban Edström^a

^a Departments of Diagnostics and Intervention, Biomedical Engineering and Radiation Physics, Umeå University, SE90187 Umeå, Sweden

^b Departments of Chemistry, Science for Life Laboratory, Umeå University, SE90187 Umeå, Sweden

^c Departments of Medical Bioscience, Pathology, Umeå University, SE90187 Umeå, Sweden

^d Departments of Applied Physics and Electronics, Umeå University, SE90187 Umeå, Sweden

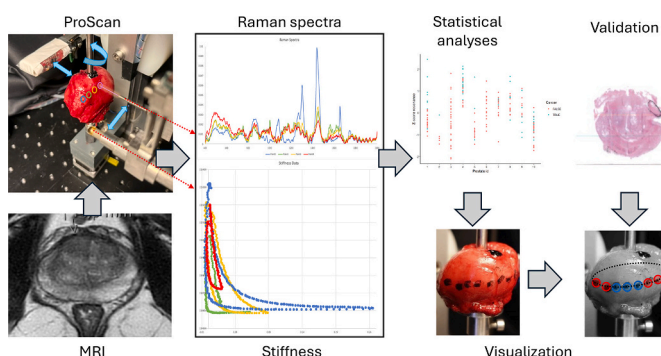
^e Departments of Diagnostics and Intervention, Urology and Andrology, Umeå University, SE90187 Umeå, Sweden

^f Departments of Public health and clinical medicine, Umeå University, SE90187 Umeå, Sweden

HIGHLIGHTS

- Cancer is assessed by Raman spectroscopy and stiffness in whole excised prostates.
- Raman and stiffness results are validated against histopathology morphometries and MRI statements.
- The method is fast and aims to provide on-site decision support during surgery.

GRAPHICAL ABSTRACT



ARTICLE INFO

Keywords:

Prostate cancer
Raman spectroscopy
Stiffness
Whole prostate
Clinical applications

ABSTRACT

Prostate cancer treatment depends on whether the cancer exists only inside the gland or within the prostate capsule or on the outside surface of the gland. The presence on the outside surface indicates migration of the cancer to adjacent organs. This study presents a novel method for detecting prostate cancer (PCa) on the surface of excised prostate glands using Raman spectroscopy and stiffness measurements. The workflow involves assessing the location and extent of PCa via MRI before surgery, followed by 3D scanning of the excised prostate. Key positions on ten excised prostates, 211 positions with 56 deemed as cancer, are measured using Raman spectroscopy and stiffness probes. The results are mapped onto a digital representation of the prostate to aid surgical decision-making. Statistical analysis of the Raman data indicates that spectra could be divided into two components, one more related to cancer and one more related to normal tissue. A stiffness parameter was calculated from resonance measurements from the stiffness probe. The Raman components and stiffness parameters were converted to z-scores. Logistic generalized linear mixed modelling revealed that the stiffness parameter was statistically associated with cancer presence in prostate regions ($p = 0.009$). The scanning

* Corresponding author.

E-mail address: olof.lindahl@umu.se (O. Lindahl).

<https://doi.org/10.1016/j.saa.2025.126992>

Received 13 May 2025; Received in revised form 26 August 2025; Accepted 23 September 2025

Available online 24 September 2025

1386-1425/© 2025 The Authors. Published by Elsevier B.V. This is an open access article under the CC BY license (<http://creativecommons.org/licenses/by/4.0/>).

equipment is easy to handle and makes further larger studies possible. This method holds promise for providing real-time support during surgery, reducing the need for post-surgical therapies and minimizing patient distress.

1. Introduction

Prostate cancer (PCa) is a prevalent male malignancy worldwide, ranking as the fourth most common cancer overall and the second most common cancer in men after lung cancer [1,2]. Despite advancements in diagnosis and treatment, PCa remains a significant cause of cancer-related deaths. Radical prostatectomy is the primary curative treatment for PCa, but incomplete removal of cancer tissue necessitates subsequent therapies in 10–20 % of cases in Sweden [3]. Prostate tumors often occur in the peripheral zone, near the capsule surrounding the prostate gland [4,5]. During surgical treatment, the surgeon strives for a negative surgical margin, i.e., a cut without cancer cells. Achieving negative surgical margins during radical prostatectomy is crucial for optimal oncological outcomes while avoiding damage to the neurovascular bundles, thereby minimizing the risk of future erectile problems and incontinence for the patient. The challenge is to secure total cancer removal and thus eliminate the risk of metastases with migrating aggressive cancer.

Currently, the standard procedure to verify negative surgical margins (i.e. successful and complete removal of all cancerous areas) involves a pathologist conducting this investigation post-surgery (usually several weeks after surgery). Determining whether the tumor has penetrated the capsule (presence of extraprostatic extensions, EPEs) and extended to the surgical margin (positive surgical margin, PSM) and thus had a chance of migrating into the surrounding tissue is crucial [6,7]. However, the current standard pathological procedure is time consuming and unnecessarily risks severe psychological strain for patients. Furthermore, in cases where the histopathological result indicates a PSM, additional intense radiation treatment and surgery or alternative treatments may be required, as there is a high risk of remaining cancer cells, risking the patient's life [6].

To make the procedure more cost- and resource-efficient for healthcare providers and less straining for patients, the presence of EPEs should be detected during surgery, as soon as the prostate is removed. Current clinically available methods for detecting and localizing cancer, such as MRI, CT and ultrasound, still fall short in terms of precision that would be necessary during the surgical procedure [8]. Thus, an instrument and method, which are small, reliable and precise enough are sorely needed to aid the surgeon during the surgical procedure. Such an instrument has been suggested to utilize e.g. Raman spectroscopy and stiffness measurements [9] immediately on the excised prostate, providing real-time information to support the surgeon in achieving complete cancer tissue removal before closing the surgery.

Stiffness changes in human tissue can indicate the presence of cancer. Usually, the tissue becomes harder or changes consistency due to tumors. This phenomenon has been used for detection of cancer in different organs and tissues e.g. breast and skin [10,11]. The standard procedure for diagnosing prostate cancer includes rectal examination, where the physician uses his finger to palpate the consistency of the prostate in search for lumpy or hard areas, potentially indicating cancer. Tactile resonance sensors can be considered analogous to human sensing in this respect, as they can be used to detect stiffness variations in soft tissue [11], such as the prostate. These sensors are based on piezoelectric elements that can be made to oscillate by an electronic feedback circuit [11]. When the sensor touches an object, the resonance frequency of the oscillating system changes. The resulting frequency shift provides information on mechanical properties, such as minute stiffness variations in tissue [12], and has been used to identify PCa in 1 cm thick prostate slices *in vitro* [13].

Raman spectroscopy is a laser-based vibrational spectroscopic technique that has been used to detect several types of cancer [14,15],

including PCa in prostate slices [9]. It is versatile, non-destructive and requires no external agents (labels, dyes or markers). As it provides a complete fingerprint of the entire chemical matrix of the sample without any need for sample preparation or alteration, it is well-suited for the chemical compositional analysis of sensitive biomedical samples. It is a rapid and relatively inexpensive analytical tool that can be easily adapted to clinical environments, as optical probes are relatively easy to keep sterile, clean, and maintain.

Except for an early study from our group related to stiffness [16], neither stiffness, nor Raman spectroscopy has been used to scan for PCa in whole (intact) prostates. There might be several reasons for the lack of such studies. Firstly, the tissue capsule of the prostate is highly fluorescent [9], making it extremely challenging to collect good quality Raman spectra from or through the surface of an intact, whole prostate. Secondly, access to clinically relevant whole prostates is severely limited since patients with known or suspected EPEs (e.g. via magnetic resonance imaging, MRI) are first subjected to measures aimed at eliminating EPEs (e.g. via radiotherapy) before surgery is performed.

Thus, the clinically most relevant samples when the cancer is detectable on the surface of the prostate are less frequently obtained. Finally, standard clinical practice limits the amount of time available for performing Raman spectroscopic measurements before the resected prostate needs to be returned to the normal clinical workflow (histopathological evaluation).

This study aims to investigate the feasibility of a setup that combines Raman spectroscopy and stiffness measurements to rapidly and non-destructively detect PCa on the surface of resected prostate glands, with hopes that such setups could become a semi-automated decision-support tool during radical prostatectomy.

2. Material and methods

Material: Ethical approval was given by the Swedish Ethical Review Authority (Dnr 2020–03649). Ten prostates were acquired, with written and informed consent, from prostate cancer patients undergoing radical prostatectomy at the University Hospital in Umeå, Sweden. The written anonymized MRI statement for each patient was used for planning the sites for measurements.

The resected prostates were immediately brought to the pathology department, where a board-certified uropathologist removed the seminal vesicles and marked the apex on the dorsal side with an ink dot for orientation purposes. Thereafter the prostates were transported on ice to the analytical laboratory.

The workflow is summarized in Fig. 1. The total time for the measurements was restricted to 1 h, after which the prostate had to be returned to the pathology lab for fixation, paraffin embedding, cutting as whole-mount sections and htx-eosin staining. This time restriction is due to current clinical practices and leads to the total number of measurement points on each prostate to be limited to ca. 20 / prostate. The number of prostates available for this study was limited (see Discussion/Conclusion).

After Raman spectroscopic and stiffness measurements, the prostate was transferred to the pathology lab, where its exterior was stained with tissue-marking dye (Triangle Biomedical Sciences, Inc. Durham, NC, USA) for histopathological analyses. Yellow ink was used at the prostate posterior, green at the front right side and red at the front left side. The ink-marking was used to determine if PSM was present. The prostates were cut into 4–5 mm thick slices horizontally, perpendicular to the rectal surface and perpendicular to the distal part of the prostatic urethra in a way that secured that the measured spots could be localized in the whole-mount sections. Each prostate slice was embedded in paraffin

and sliced in 4- μm thin slices [9]. The histological analysis followed standard clinical routine at the pathological department (Fig. 2) and was used together with the MRI-statement (Fig. 3, Table 1) to determine and verify the location of cancer in the prostate, see Fig. 2).

3. Methods

3.1. Equipment

An in-house developed scanning and rotating device (ProScan, Swedish Patent SE 546317 C2) (Fig. 4) was used to scan the prostate with a fiber-optic Raman probe and a stiffness probe. The small diameter probes (Raman: 1 mm; stiffness: 5 mm) were housed in a mounting frame with a fixed distance between them, allowing for automated swapping of the probes while retaining the sample position. The housing was attached to a motorized 3D ruler, maneuvered by custom developed software written in LabView™. The setup allows for rotating and tilting the prostate gland, making about 90 % of the surface accessible to both Raman spectroscopic and stiffness measurements. In-house developed software was used to scan the prostate in 3D and direct the measurements to user-defined spots on the surface of the gland (Fig. 4).

3.2. Raman spectroscopy

Raman spectroscopic measurements were carried out using a custom-built spectrometer by EMVision (EMVision LLC, Loxahatchee, Florida, USA), employing a 785 nm laser through a fiber optic probe with a 1 mm diameter tip. The probe was designed for the tip to be in direct contact with the sample surface. Spectra were recorded over the fingerprint region (277–2008 cm^{-1}) at a constant laser power, limited to 40 mW, on the sample surface. The laser power was measured at the probe exit using a handheld digital optical power and energy meter (C series, Thorlabs Sweden AB, Mölndal, Sweden) at the start of every measurement. Depending on signal strength and fluorescence levels at each spot on the prostate, exposure times were allowed to vary between 1 and 10 s, to maximize signal to noise ratio in the resulting spectra. These parameters were first verified to be safe during test runs, and no visible or spectral drifts or changes were observed at any point on the prostate samples during measurements that would have indicated the laser power levels affecting the sample. Also, the following

morphometric investigations did not indicate laser-induced deviations.

3.3. Stiffness

The stiffness measurements were conducted using an in-house-made resonance sensor system, following the principle described earlier [9,17]. In short, the stiffness sensor was made of PZT (Lead Zirconate Titanate) and shaped as a cylinder (5 mm outer diameter, 3 mm inner diameter, 20 mm length). The PZT was provided by Morgan Electro Ceramics (Bedford, OH, USA) and the driving electronics for the PZT were designed and developed in-house. The probe tip was hemispherical with a 2,5 mm radius. Stiffness sensing with a resonance sensor has been described in detail previously [18–20]. A double-bending beam force sensor (Fig. 4) was used to detect the contact force when touching the object under investigation. Tissue impression depth was set to be 2 mm, and the output was the stiffness parameter, defined as $\partial\Delta f/\partial F$ (f[Hz], F [N]) [9,17].

3.4. Data analysis

The histopathological and MRI data were used to define the positions of cancer tumors in the prostate gland in relation to the measured data points. Photographs of the prostate gland mounted on the ProScan with ink dots showing the sensor positions (Fig. 2 left) could be aligned with the morphometric data (Fig. 2) and finally compared with MRI data (Table 1).

Spectra were calibrated using tylenol (paracetamol, N-(4-hydroxyphenyl)acetamide, N-(4-hydroxyphenyl)ethanamide) bands by the Python-based ORLP-GUI (<https://github.com/mr-sheg/orpl>) and exported as ASCII text files. The text files were processed by a MATLAB (Mathworks Inc., USA)-based, free, open-source graphical user interface available through the Vibrational Spectroscopy Core Facility at Umeå University (<https://www.umu.se/en/research/infrastructure/visp/>, as initially documented by J. Felten et al. [22]). Spectral processing steps included cutting the spectra to the 400–2000 cm^{-1} region, followed by asymmetrical least squares baseline correction [23] with $\lambda = 10,000$ and $p = 0.001$, Savitzky-Golay smoothing [24] using a first order polynomial and a frame of five, and total area normalization over the entire cut spectral area. Multivariate Curve Resolution – Alternating Least Squares [25] was performed on the processed data, with 2

Flow chart

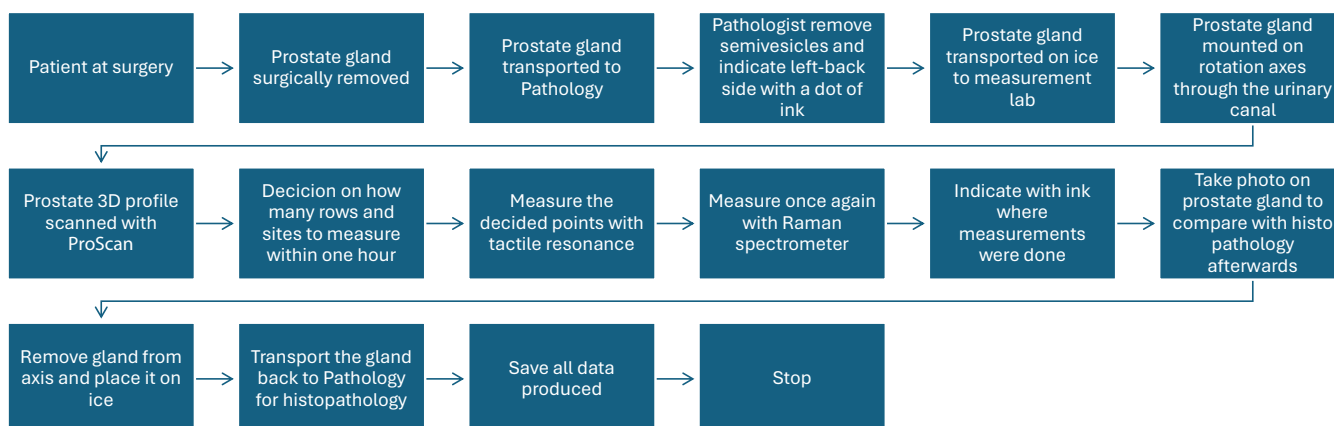


Fig. 1. Measurement workflow.

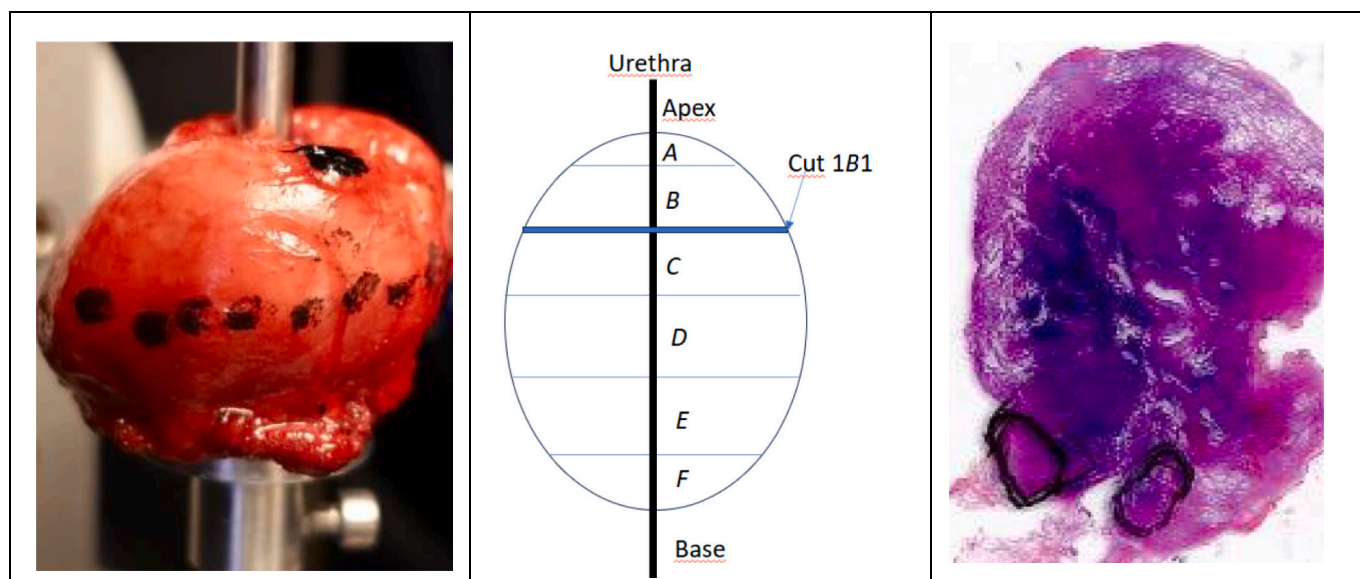


Fig. 2. Left: Actual positions for measurements, indicated with ink dots (after the measurements). Middle: Schematic drawing showing the location of slices (cut) used by the pathologist to indicate location of morphometric findings. Right: A single slice for histopathological examination of cancer presence by a trained pathologist (black rings indicate tumor areas).

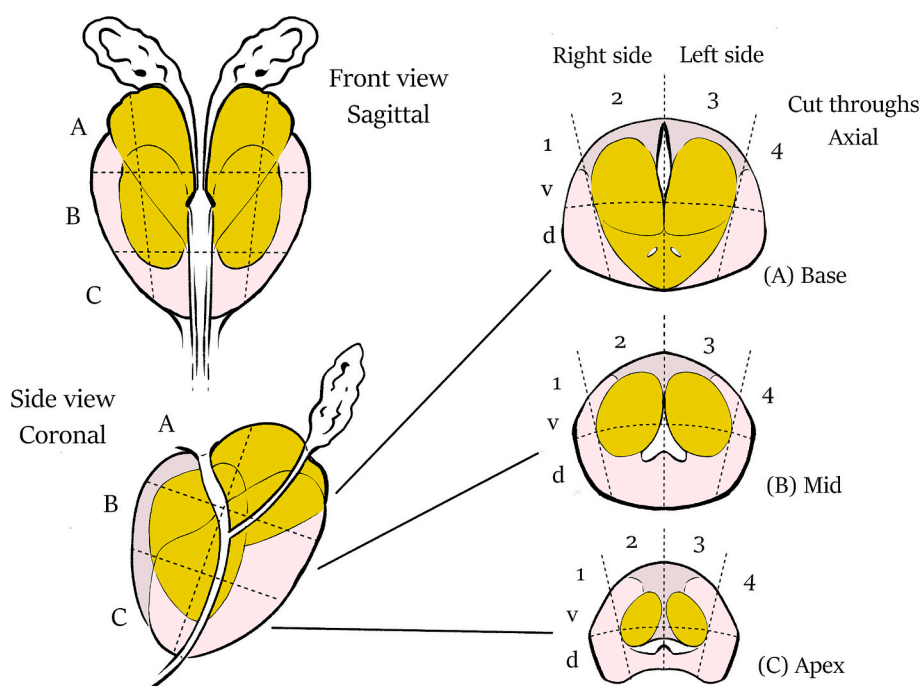


Fig. 3. Schematics for orientation and sectioning of the prostate used by the radiologists to define where tumors were found (Table 1).

components (based on the working hypotheses that cancerous and cancer-free areas would have different spectral profiles), using all 182 recorded spectra, with SIMPLISMA-based initial estimates as starting points. Only concentration and spectral non-negativity constraints were employed. Convergence (0.1 % sigma change) was achieved in 13 iterations, explaining 97 % of the variance in the data.

3.5. Statistical analyses

As the distribution of the stiffness parameter was negatively skewed, the values were transformed by first multiplying them by -1 , and thereafter logarithmized and converted into z-scores by subtracting the

mean and dividing by the standard deviation across all measured ROI [17]. This was done to facilitate interpretation of the stiffness parameter; one unit of the z-score corresponds to one standard deviation on the log-scale. A larger z-score implies a less stiff tissue. Z-scores were also calculated for Raman component 1 on the log scale and for Raman component 2 on its original scale (i.e. no log transformation). Associations between the stiffness z-score and the Raman component 1 and 2 z-scores, respectively, were graphically visualized. Further, the association was tested using a mixed effect model with stiffness z-score as dependent variable and component 1 and 2 z-scores, respectively, as independent variable. Z-scores Raman components 1 and 2, respectively, were included as fixed effects, in two separate models, and

Table 1

MRI statement for the prostates before surgery concerning volume of whole prostate, location of tumor in prostate according to Fig. 3 and the probability of cancer expressed as standard PIRADS [21]. EPE indicates suspected extra prostatic extension, i.e. tumor penetrating the prostate capsule. Locations of cancer were further referenced against histopathological data, see Fig. 2.

| Prostate number | Volume ml | Location | PI-RADS |
|-----------------|-----------|-------------------------|---------|
| 1 | 46 | 3 Bd | 4 |
| 2 | 26 | 1Cd, 1B/Cd | 4 |
| 3 | 25 | 4Av (EPE2), BH2 | 4 |
| 4 | 86 | 1/2C/Bv | 5 |
| 5 | 57 | 2ABv (EPE), 4ABdv (EPE) | 4–5 |
| 6 | 48 | 1/2Bv, 1/2 Bd | 3 |
| 7 | 40 | Unclear | 2 |
| 8 | 47 | C3v/d, B3v/d | 3 |
| 9 | 80 | 1 Bd, 2 Bd, 1Bv (EPE) | 5 |
| 10 | 47 | 2 Bd, 2Cd, 3 Bd | 4 |

random intercept and random slope were included for the effect to account for the repeated measurements on the same prostates.

Associations between occurrence of cancer tissue and stiffness z-score, and Raman component 1 and 2 z-scores as dependent variables, respectively, were investigated using generalized linear mixed models (GLMM) with a logit link function, including random slopes and intercept for prostate. Mixed models [26] were used for handling the dependence between observations within the same prostate. The mixed models approach was previously employed for this purpose, using Raman and stiffness data (see Ref. [17]). The odds ratio for the ROIs being cancer tissue was estimated from the GLMM, with 95 % confidence interval. An odds ratio greater than 1 implies an increasing risk of being cancer as the dependent variables increase.

The R-package glmmTMB [27] was used to fit the mixed effects models using restricted maximum likelihood. Further, in a separate model, the joint effect of modelling cancer occurrence from both resonance and Raman measurements in the same model were investigated by including both the stiffness Z-score and the Raman component 1 as independent variables with random intercepts for prostates.

Further, we also investigated the associations between certain positions on the Raman spectra and occurrence of cancer, using the previously described random intercept and random slope GLMM, with cancer occurrence and Raman intensity as independent variable.

All statistical analyses were performed using R version 4.3.1 [28].

4. Results and discussions

4.1. Raman spectroscopy

Raman spectroscopy provides a viable option for real-time assistance for surgical decision-making with respect to finding cancer on the surface of freshly removed prostate (i.e. probing for positive surgical margins). It is fast, non-destructive, relatively inexpensive, and requires no external agent (label, dye or marker) and thus it is non-invasive. In addition, it is portable and easy to clean and sterilize, making it easy to adapt to surgical settings. Crucially, it has been proven capable of identifying cancer in prostate tissue [8].

However, applying it to whole prostates and especially through the tissue capsule is less than straightforward and has not been attempted in direct connection with surgeries. Major concerns arise due to fluorescence disturbances from the tissue capsule, which can disturb (or completely overwhelm) the vibrational bands needed for the analysis. In addition, according to the ethical approval for this study, the clinical setting-imposed constraints as the measurements had to confine to the established clinical practice completely. This limited the time available for measurements.

To facilitate rapid and accurate scanning and future visualization of the results (for evaluation and validation purposes), a novel scanner setup (ProScan) was used. It consists of a stainless-steel pole with a lock-in disk at the base for mounting the prostate (through the urinary channel) and connected precise, computer-controlled stepper motors to allow rotation around the pole axis and wagging perpendicular to the pole axis. This setup enables the three-dimensional rotation of the prostate, which – together with a proximity sensor- allows for a complete scanning of the prostate surface and its 3D computer representation. The computer can then mark points on the surface of the prostate for measurements and rotate the prostate to any of the points selected by the operator to perform measurements. The ProScan setup also includes two probes, side-by-side, for stiffness measurements and fiber-optic Raman spectroscopy, which are aligned so that the operator can switch between them and maintain the position of the prostate selected for investigations. This setup speeds up the workflow so that within 1 h (the time allowed to pass between the surgical removal of the prostate and its transfer for histopathology), more than 20 points can be recorded by both stiffness measurements and Raman spectroscopy. While this number of points still requires careful consideration of measurement areas (i.e. focusing on areas that are more likely to contain cancer, as the entire prostate surface cannot be mapped in this time), it provides enough observations for statistical analyses.

Based on the MRI statements, we recorded a different number of points from 10 prostates ($n = 178$), with a different proportion of the

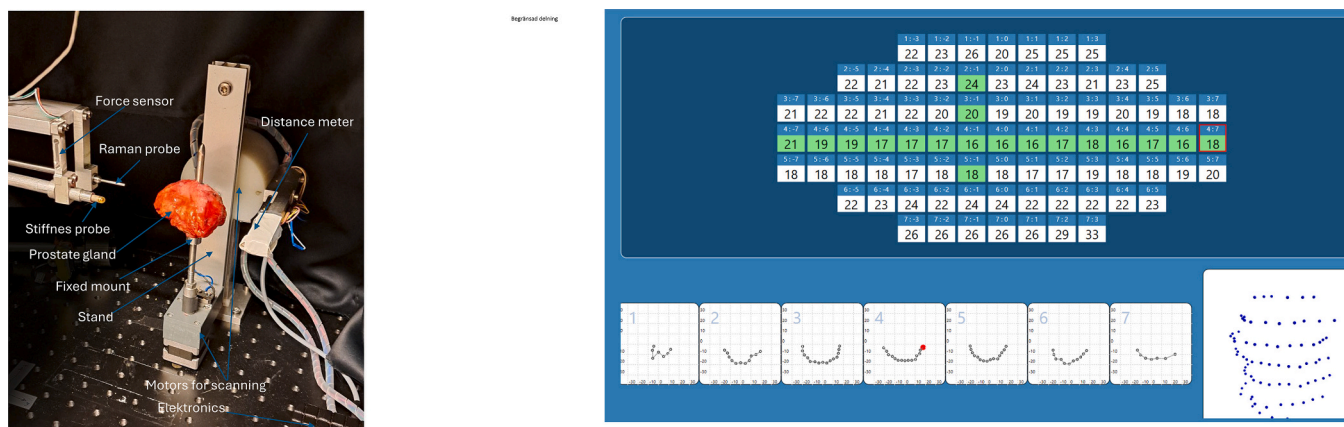


Fig. 4. Left: The ProScan experimental setup, with a newly resected prostate gland mounted for scanning. Right: Controlling software for 3D scanning and measurement position layout.

recorded positions adjudged to contain cancer in each prostate. The number of points per prostate varied also because of the varying exposure times in Raman spectroscopic measurements, that were needed to ensure maximum signal intensity without altering the sample. Thus, areas with uneven surfaces producing low Raman signal had to be measured longer, as the laser intensity cannot be increased beyond limits deemed safe).

Points for measurements (both Raman and stiffness) were selected to maximize the chances of recording both cancer and non-cancer areas. MRI statements were used for general orientation, and the opinions of the surgeon were taken into consideration as well. Thus, areas with suspected cancer were covered as much as possible, including surroundings to outline any potential spread, as well as areas deemed cancer-free, for control.

However, no selection procedure, no matter how carefully done, can guarantee a 100 % success in recording both cancer and non-cancer areas of any given prostate. This is due to another constraint from the clinical practice, which lies in the fact that the surgical removal of the prostate is done primarily on patients where the potential of EPE is low, and naturally the surgeons aim to have negative surgical margins. Thus, the number of points with cancer on the surface of the prostate is going to be far lower than the number of cancer-free positions, and at times no cancer will be found on the surface. This is naturally good news for the patient, but in a technical sense, it skews statistical analyses and limits the sensitivity towards cancer profiles (as such profiles will be based on fewer observations). Moreover, there is often no clear visible indication as to where exactly any potential EPE is located on the prostate, only a general approximation to a larger area / side of the prostate. Since the Raman fiber optic probe has a spot size of approximately 1 mm in diameter, it is very easy to miss actual EPE spots even if the larger general area on the prostate is correctly identified. This further limits the number of actual cancer data recorded among the ten prostates used in this study.

The stiffness probe is less sensitive to such locational / positional misses, since it is larger and thus probes a larger area, and it probes deeper [17] than the Raman laser (which is more focus / surface sensitive). Thus, in cases when the cancer lies deeper (negative surgical margin), the stiffness probe can still “sense” it more than the Raman spectral probe does.

Keeping these limitations in mind, we subjected the Raman spectra to multivariate curve resolution using alternating least squares (MCR-ALS). Instead of aiming for “pure” chemical compounds, or even classes of compounds (such as fatty acids, proteins, etc.) as components, we selected two components, which we hoped to correlate to cancerous and non-cancerous areas. The basis of this assumption was the fact that non-cancerous areas were expected to show considerable fluorescence from the tissue capsule. Cancer that has broken through the tissue capsule, on

the other hand, was expected to show Raman spectral bands matching those recorded from tissue sections and cell cultures of prostate cancer, such as shown in e.g. [8]. In other words, the largest variation in the dataset is not expected to come from a diagnostic chemical compound that only exists in cancer cells and has a distinct Raman spectral profile. Instead, the basic building blocks of cancerous and normal prostate cells (proteins, lipids, nucleic acids, ...) are expected to be largely similar, with certain ratios / proportions among them expected to change. In addition, band shifts are possible as well, due to e.g. potential protein compositional and/or 3D structural changes, or as a result of the overall chemical matrix changing. Therefore, aiming to resolve individual classes of chemical compounds would be unrealistic in this dataset, and would miss the primary goal of the analysis, i.e. finding distinctive descriptors for cancerous and non-cancerous areas.

The results (Fig. 5, Supplementary File 1) show that resolved profiles fit the expectations: one of them contains bands strikingly similar to those of prostate cancer recorded from sections and cell cultures, while the other has broader, less well-defined spectral features as the high contribution of fluorescence diminishes the Raman signals (see spectra provided in Supplementary File 1).

4.2. Stiffness measurement

Linear mixed models revealed a statistically significant association between Stiffness parameter and Raman component 1 ($\beta = 0.32$, 95 % CI: [0.02, 0.61], $p = 0.037$). This should be interpreted as an expected 1 unit in Raman component 1 leads to an increase of 0.37 standard deviations of the stiffness parameter, on the logarithmic scale. However, the association was weak, as revealed when visualizing in scatter plots (Fig. 6).

The stiffness parameter was statistically significantly associated with the presence of cancer tissue (odds ratio (OR) = 3.41, 95 % CI: [1.36, 8.60], $p = 0.009$). The OR should be interpreted as the multiplicative change in odds for tissue being cancer for a unit increase in standard deviation in Stiffness parameter, i.e. for an increase of one standard deviation in stiffness parameter, the expected odds for the investigated ROI being cancer tissue increases 3.41 times. This indicates that the stiffness parameter may be used as a predictor for cancer (confirming earlier results, e.g. [17]). However, predictive abilities could not be tested on the current dataset, due to the low number of prostates that could be tested during reasonable time. Every prostate measurement under the current ethical approval involved advanced logistics as described in the methods section. Raman component 1 z-score, on the other hand, was not statistically significantly associated with the presence of cancer tissue (OR = 1.91, 95 % CI: [0.60, 6.05], $p = 0.274$). (See Fig. 7 for graphical representations).

In a likelihood-ratio test, the improvement in goodness of fit was not

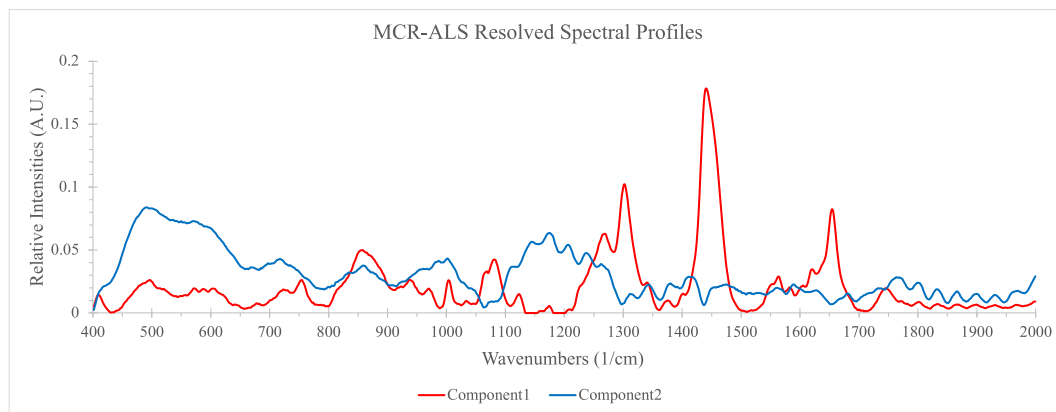


Fig. 5. MCR-ALS resolved Raman spectral profiles for a 2-component model. Component 1) contains bands matching the spectral signature of prostate cancer from tissue sections and cell cultures. Component 2 contains broad features, plagued by fluorescence.

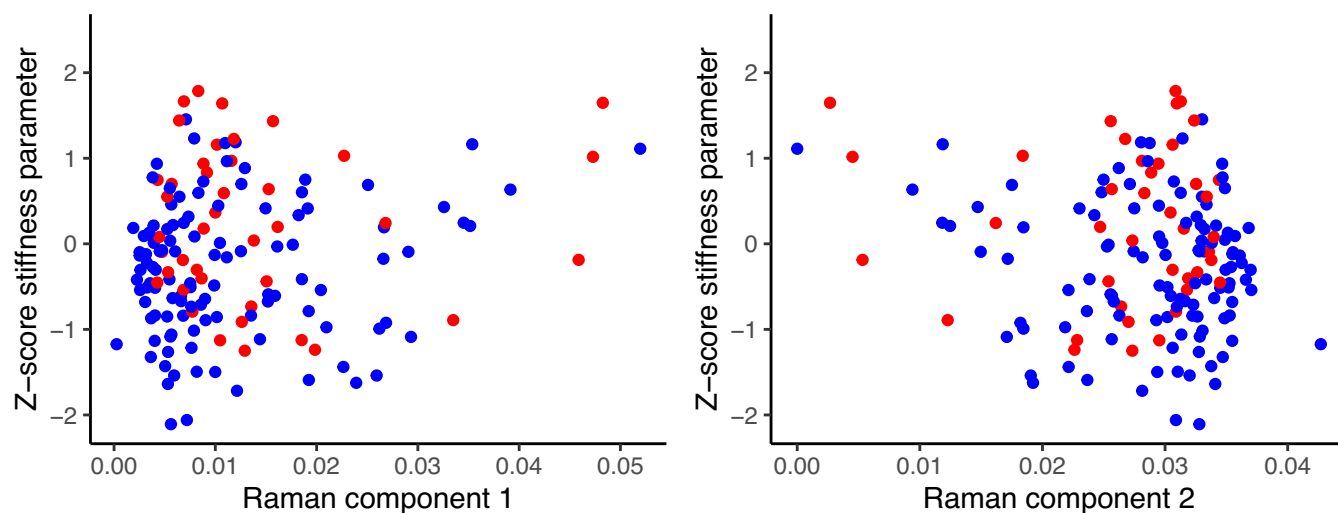


Fig. 6. Relations between MCR-ALS resolved Raman components and Z-score stiffness parameter. Red dots represent cancer; blue dots represent non-cancer points in the prostate. (For interpretation of the references to colour in this figure legend, the reader is referred to the web version of this article.)

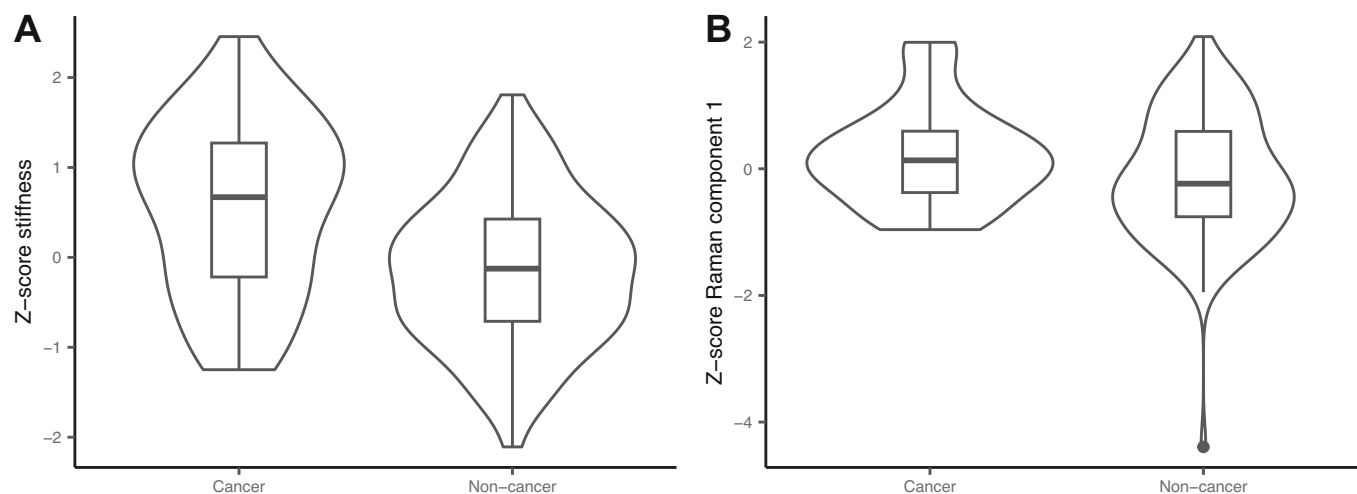


Fig. 7. Violin plot and boxplot comparing Z-score stiffness parameters and Raman component 1 between cancer and non-cancer tissues. The boxes represent the interquartile range (IQR; 25th to 75th percentile), with the horizontal line indicating the median. Whiskers extend to the most extreme data points within 1.5 times the IQR from the quartiles. No points beyond 1.5 IQR were present.

statistically significant when comparing a mixed-effects model with both the stiffness parameter and Raman component 1 as fixed effects to a model using only the stiffness parameter. This provided no evidence that including Raman data would improve the model compared to using only the stiffness parameter as the dependent variable. However, note that the sample size is small; from the 10 prostates, out of 211 examined regions, only 56 were deemed as cancer tissues. Thus, we have low statistical power and possible sparse data bias. Convergence problems were reported for all GLMM models. However, the stiffness data have predictive qualities as already mentioned and the Raman spectra could be divided into two profiles, one more related to normal tissue and one more related to cancer tissue, indicating that in a larger study stiffness and Raman spectra combined may give a more secure detection of cancer cells. For future studies with the aim of assessing the predictive performance of stiffness and Raman spectral profiles for identifying cancer tissue, considerably more data is needed. To test whether certain bands previously found in the Raman spectra of cancerous tissue sections could improve the models, we performed a similar test, simply using band intensities at a given wavenumber (the centre of the band). However, there were no statistically significant associations between these specific Raman bands and cancer in our dataset (Fig. 8).

4.3. Combining Raman spectra and stiffness data

It has already been suggested that both stiffness measurement and Raman spectra have the potential to detect cancer in prostate [8,9,17] and it has further been confirmed here. However, both techniques have drawbacks. Raman spectra are sensitive to fluorescence and experience difficulties when detecting chemical compounds in highly fluorescent materials such as prostate tissue. Raman spectra are collected from the surface in our setup, as we are primarily probing for EPEs, but cancer tumors are often located deeper in the tissue. Stiffness measurements, on the other hand, are sensitive to hard non-cancerous structures in the tissue, like prostate stones, that can be wrongly detected as cancer tumors [9], i.e. false positives. The stiffness measurement is also more in depth, detecting stiffer structures down to 5–6 mm in the tissue [16]. Our idea, based on the ProScan, is to combine the two methods and first detect stiff nodules by stiffness measurements and then use Raman spectra to detect the chemical compounds related to cancer in the identified nodules, and see if any of the cancer can be detected on the surface (EPE, positive surgical margins). The aim is to securely detect cancer on the surface of the prostate gland by our ProScan setup with high enough accuracy to become clinically reliable. Thereby, it could

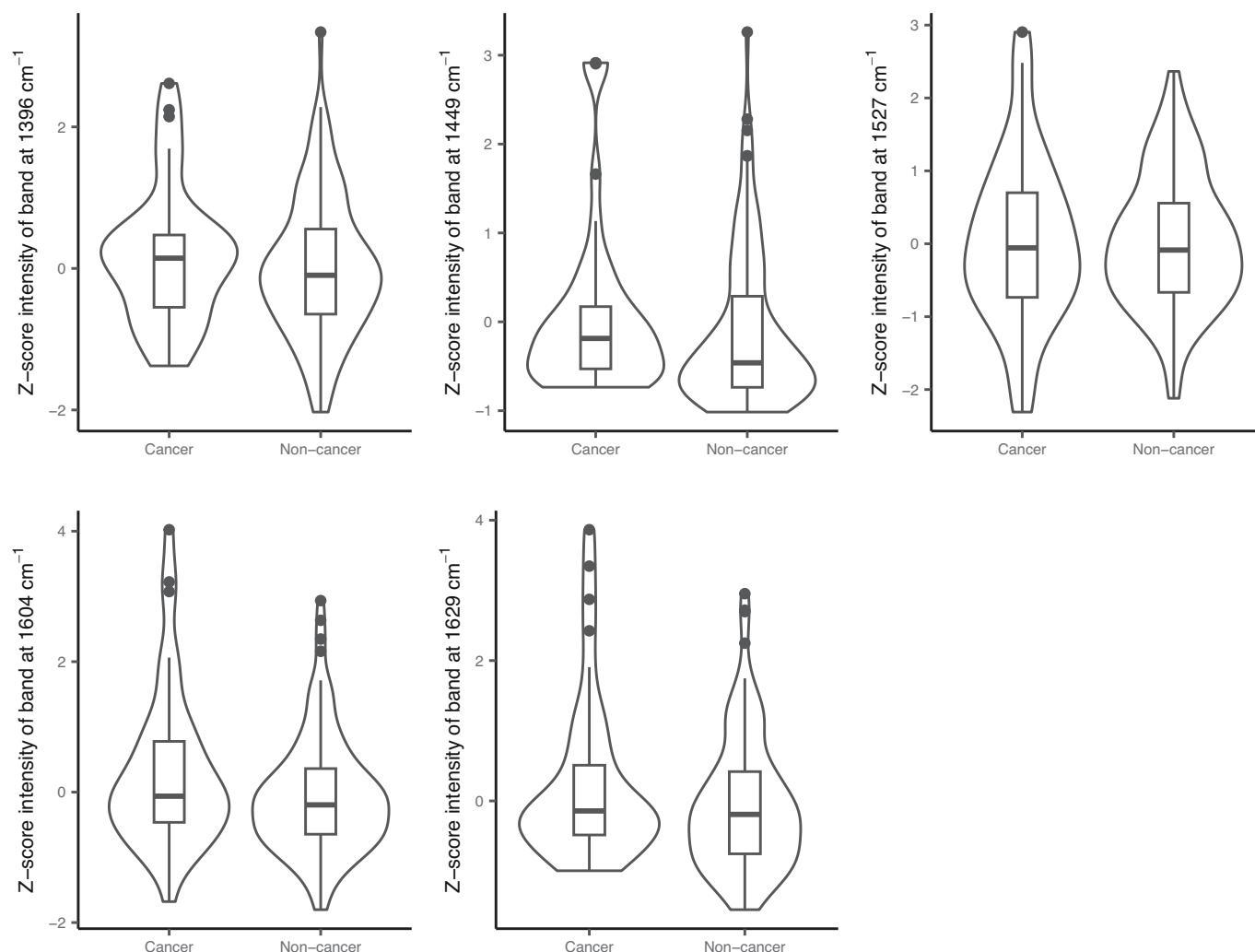


Fig. 8. Violin plot and boxplot of intensities of difference Raman bands between cancer and non-cancer tissues. The boxes represent the interquartile range (IQR; 25th to 75th percentile), with the horizontal line indicating the median. Whiskers extend to the most extreme data points within 1.5 times the IQR from the quartiles. Observations beyond 1.5 IQR are represented by points.

provide on-site decision support to the surgeon for nerve and vessel sparing surgery and successful (i.e. complete) removal of prostate cancer. Such surgical decisions support is currently unavailable via the golden standard for precise localization of cancer in prostate tissue, i.e. histopathology, as that route demands a trained pathologist as well as laboratory facilities and time (for sectioning, staining and assessment) that cannot easily be introduced in the operating room within the time frame of the surgery.

5. Conclusion

We have developed a method to detect prostate cancer on the surface of an excised prostate. The developed hardware (ProScan) gives the possibility to measure a whole prostate relatively quickly and give precise information about stiffness and Raman spectra at specific sites on the prostate. This technique has not been demonstrated before. The dual sensing tools attached to ProScan (stiffness and Raman fiber optic probes) allow for independent, multi-method data to be collected at every point on the prostate surface.

Stiffness measurements have shown statistically significant prediction of superficial cancer on the prostate surface as compared with standard clinical tools (MRI, histopathology).

Raman spectra could be divided into two profiles, one more related to cancer and one more related to normal prostate tissue. While

statistically significant cancer associations could not be found in this dataset, it seems reasonable to expect that more data would reinforce associations.

We note that the ProScan also gives a unique possibility to perform much larger, semiautomatic studies in the future at a higher speed.

With a larger sample set, and ethical allowance for greater flexibility for non-standard measurements, such as ProScan mounted stiffness and Raman spectral data collections, will improve the method.

We emphasize that the aim is not to replace pathological verifications, but to provide real-time, on-site aid to detect cancer during surgeries. On larger datasets, artificial intelligence / machine learning training can further mine the Raman spectral data as well, further improving the methods capacity to identify potential positive surgical margins, or at least improve automation and speed.

Funding sources

The study has received grants from Swedish Governmental Agency for Innovation Systems, Medtech4-Health (grant number 2022-03184) and from the Swedish foundation Kempestiftelserna.

Declaration of competing interest

The authors declare that they have no known competing financial

interests or personal relationships that could have appeared to influence the work reported in this paper.

Acknowledgements

The authors wish to express their gratitude to Kerstin Almroth, research assistant at the Department of Diagnostics and Intervention, Umeå University and Pernilla Andersson, research assistant at the Department of Medical Bioscience at Umeå University for skillful laboratory assistance. We further wish to thank Tobias Nordin, Nordink Company, for skillful graphical illustration in Fig. 3.

The Vibrational Spectroscopy Core Facility at Umeå University gratefully acknowledges the support received via the Chemical Biological Centre (KBC) and the Department of Chemistry, at Umeå University.

Appendix A. Supplementary data

Supplementary data to this article can be found online at <https://doi.org/10.1016/j.saa.2025.126992>.

Data availability

Data will be made available on request.

References

- [1] F. Bray, J. Ferlay, I. Soerjomataram, R.L. Siegel, L.A. Torre, A. Jemal, Global cancer statistics 2018: GLOBOCAN estimates of incidence and mortality worldwide for 36 cancers in 185 countries, *CA Cancer J. Clin.* 68 (6) (2018) 394–424.
- [2] P. Rawla, Epidemiology of prostate cancer, *World. J. Oncol.* 10 (2) (2019) 63–89.
- [3] B. Djavan, et al., European study of radical prostatectomy: time trends in Europe, 1993–2005, *BJU Int.* 100 (Suppl. 2) (2007) 22–25.
- [4] N. Samavati, D.M. McGrath, M.A.S. Jewett, T. van der Kwast, C. Ménard, K. K. Brock, Effect of material property homogeneity on biomedical modeling of prostate under deformation, *Phys. Med. Biol.* 60 (2015) 195–209.
- [5] D. Colleselli, D. Schilling, M.P. Lichy, J. Hennenlotter, U.H. Vogel, S.A. Kreuger, et al., Topographical sensitivity and specificity of endorectal coil magnetic resonance imaging for prostate cancer, *Urol. Int.* 84 (2010) 388–394.
- [6] S. Adamis, I.M. Varkarakis, Defining prostate cancer risk after radical prostatectomy, *Eur. J. Surg. Oncol.* 40 (2014) 496–504.
- [7] O. Yossepowitch, A. Bjartell, J.A. Eastham, M. Graefen, B.D. Guillonéau, P. I. Karakiewicz, et al., Positive surgical margins in radical prostatectomy: outlining the problem and its long-term consequences, *Eur. Urol.* 55 (2009) 87–99.
- [8] K. Aubertin, et al., Mesoscopic characterization of prostate cancer using Raman spectroscopy: potential for diagnostics and therapeutics, *BJU Int.* 122 (2) (2018) 326–336.
- [9] M. Nyberg, V. Jalkanen, K. Ramser, B. Ljungberg, A. Bergh, O.A. Lindahl, Dual-modality probe intended for prostate cancer detection combining Raman spectroscopy and tactile resonance technology—discrimination of normal prostate tissue ex vivo, *J. Med. Eng. Technol.* 39 (2015) 198–207.
- [10] O.A. Lindahl, et al., Tactile resonance sensors in medicine, *J. Med. Eng. Technol.* 33 (4) (2009) 263–273.
- [11] O.A. Lindahl, S. Omata, K.A. Angquist, A tactile sensor for detection of physical properties of human skin in vivo, *J. Med. Eng. Technol.* 22 (4) (1998) 147–153.
- [12] S. Omata, Y. Terunuma, New tactile sensor like the human hand and its applications, *Sensors Actuators* 35 (1992) 9–15.
- [13] V. Jalkanen, et al., Resonance sensor measurements of stiffness variations in prostate tissue in vitro—a weighted tissue proportion model, *Physiol. Meas.* 27 (12) (2006) 1373–1386.
- [14] K. Eberhardt, et al., Advantages and limitations of Raman spectroscopy for molecular diagnostics: an update, *Expert. Rev. Mol. Diagn.* 15 (6) (2015) 773–787.
- [15] K. Kong, et al., Raman spectroscopy for medical diagnostics—from in-vitro biofluid assays to in-vivo cancer detection, *Adv. Drug Deliv. Rev.* 89 (2015) 121–134.
- [16] A.P. Åstrand, et al., Prostate cancer detection with a tactile resonance sensor—measurement considerations and clinical setup, *Sensors (Basel)* 17 (11) (2017) E2487.
- [17] O.A. Lindahl, et al., A tactile resonance sensor for prostate cancer detection—evaluation on human prostate tissue, *Biomed. Phys. Eng. Express.* 7 (2) (2021) 025004.
- [18] S. Omata, Y. Terunuma, Development of new type tactile sensor for detecting hardness and/or softness of an object like the human hand, in: *Proc 6th Int Conf Solid-State Sensors and Actuators*, 1991. San Francisco, CA, USA.
- [19] V. Jalkanen, et al., Prostate tissue stiffness as measured with a resonance sensor system: a study on silicone and human prostate tissue in vitro, *Med. Biol. Eng. Comput.* 44 (7) (2006) 593–603.
- [20] Y. Murayama, O.A. Lindahl, Sensitivity improvements of a resonance-based tactile sensor, *J. Med. Eng. Technol.* 41 (2) (2017) 131–140.
- [21] B. Turkbey, et al., Prostate imaging reporting and data system version 2.1: 2019 update of prostate imaging reporting and data system version 2, *Eur. Urol.* 76 (3) (2019) 340–351.
- [22] J. Felten, et al., Vibrational spectroscopic image analysis of biological material using multivariate curve resolution—alternating least squares (MCR-ALS), *Nat. Protoc.* 10 (2) (2015) 217–240.
- [23] P.H.C. Eilers, Parametric time warping, *Anal. Chem.* 76 (2) (2004) 404–411.
- [24] A. Savitzky, M.J.E. Golay, Smoothing and differentiation of data by simplified least squares procedures, *Anal. Chem.* 36 (8) (1964) 1627–1639.
- [25] J. Jaumot, et al., A graphical user-friendly interface for MCR-ALS: a new tool for multivariate curve resolution in MATLAB, *Chemom. Intell. Lab. Syst.* 76 (1) (2005) 101–110.
- [26] J.J. Faraway, *Extending the Linear Model with R: Generalized Linear, Mixed Effects and Nonparametric Regression Models*, Chapman and Hall/CRC, 2016.
- [27] M.E. Brooks, K. Kristensen, K.J. van Benthem, A. Magnusson, C.W. Berg, A. Nielsen, et al., glmmTMB balances speed and flexibility among packages for zero-inflated generalized linear mixed modeling, *R J.* 9 (2) (2017) 378–400.
- [28] R Core Team, *R: A Language and Environment for Statistical Computing*, R Foundation for Statistical Computing, Vienna, Austria, 2023.